Chemical Engineering Journal 94 (2003) 11–18

Chemical Engineering Journal

www.elsevier.com/locate/cej

# Kinetic investigations on the oxidehydrogenation of propane over vanadium supported on γ-$Al_2O_3$

Aldo Bottino [a], Gustavo Capannelli [a,*], Antonio Comite [a], Silvia Storace [a], Renzo Di Felice [b]

[a] *Dipartimento di Chimica e Chimica Industriale, Università degli Studi di Genova, Via Dodecaneso 31, 16146 Genova, Italy*
[b] *Dipartimento di Ingegneria Chimica e di Processo "G. Bonino", Università degli Studi di Genova, Via Opera Pia 15, 16145 Genova, Italy*

Received 22 May 2002; accepted 29 November 2002

**Abstract**

This work deals with the experimental determination of the reaction kinetic of the oxidative dehydrogenation (ODH) of propane and the evaluation of possible competitive reactions. The reaction network, composed of consecutive and simultaneous reactions, with kinetics expressed through simple power law equations, involves 18 unknown variables (12 order of reaction and 6 kinetic constants). They were determined through non-linear regression analysis. The overall reaction scheme was broken up for convenience and the three sub-schemes were separately investigated. Experimental measurements were carried out in a isothermal differential quartz reactor by varying the ratio between carbon compound (propane, propylene or CO) and oxygen. The chosen operating conditions proved the system was working in kinetic controlling conditions in the temperature range of 653–753 K. A simple rate equation that assumed the reactant adsorption, reaction on the catalyst surface and re-oxidation of the active site through molecular oxygen was used.


*Keywords:* Catalytic reactor; Propane oxidehydrogenation; Kinetic; Redox mechanism

## 1. Introduction

Some important processes such as ammoxidation of propylene to acrylonitrile, epoxidation of propylene or ethylene and the oxidation of propylene to acrolein produce highly desirable chemical intermediates from light olefins [1]. Nowadays, light olefins are obtained by processes such as steam cracking and fluid catalytic cracking of light oil fractions [2] or catalytic dehydrogenation. These processes are endothermic and operate under very severe conditions (high temperature and low contact time) with a subsequent high energy consumption. Their process yields are strongly influenced by the operating conditions (feed, hydrocarbon–water ratio, temperature and contact time). Numerous by-products are also obtained (with subsequent high separation costs) and the catalyst must be frequently regenerated owing to coke deposition. The demand of each olefin [3] is growing at different rates (e.g. the demand of propylene is foreseen to overtake that of ethylene). Therefore, there is a need to develop new specific processes, with lower costs and a reduced environmental impact.

Although the oxidative dehydrogenation (ODH) of paraffins for the production of light olefins (ethylene, propylene or butenes) continues to be of interest at laboratory research level, industrial applications are still hindered by unsatisfactory yields (due to the formation of carbon oxides) and technical conditions (flammability of the reaction mixture and reactor choice) [4].

The catalysts generally employed [5] are based on vanadium and the majority of studies concern their preparation, evaluation of performance in terms of the selectivity–conversion trend and correlation among catalytic activity, vanadium co-ordination and surrounding environment [6,7]. There are several papers that deal with the determination of the kinetic parameters of reactions involved in the ODH process and several mechanism pathways have been proposed [8–18]. However, little research has been done on the catalytic system V/γ-$Al_2O_3$ from a kinetic point view.

We studied a vanadium catalyst supported on alumina (γ-$Al_2O_3$). This catalyst presents lower yields than those of other catalysts studied in the past, but it has the great advantage that it limits the formation of oxygenated secondary products (e.g. acrolein and acrylic acid), which are also difficult to separate [19]. This work investigates the kinetic of the oxidative dehydrogenation of propane, taking into account the reaction network reported in Fig. 1. The reaction

* Corresponding author. Tel.: +39-010-353-6197; fax: +39-010-353-6199.
*E-mail address:* capannel@chimica.unige.it (G. Capannelli).

1385-8947/03/$ – see front matter © 2003 Elsevier Science B.V. All rights reserved.
doi:10.1016/S1385-8947(03)00003-2

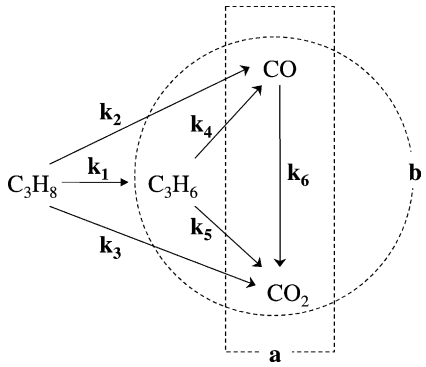


Fig. 1. Reaction network used for the kinetic and its division in the sub-schemes (a) and (b).

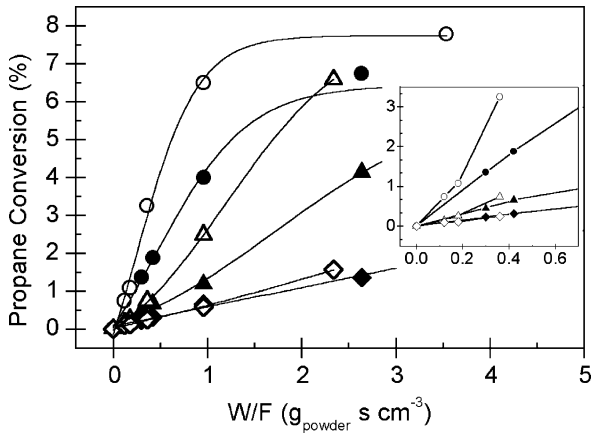


Fig. 2. Propane conversion as a function of contact time (calculated with respect to the weight of the catalytic powder in the reactor) for a packed bed volume $V$ (full symbols) and $3V$ (empty symbols) at the three temperatures investigated: 400 °C (◆, ◇); 450 °C (▲, △); 480 °C (●, ○). The small window shows an enlargement at low contact time.

scheme chosen shows the complex kinetic relationships for each of the species taking part in the process (Fig. 1), with many numerical parameters to be determined from the same experimental information. As suggested by Fogler [20], it was decided to subdivide the overall scheme into simpler sub-schemes, namely carbon monoxide combustion and propylene combustion, and then plug their kinetic results into the general scheme.

## 2. Experimental

Experimental runs were carried out in a temperature range of 653–753 K, in order to avoid simultaneous homogeneous reactions, which can occur above 773 K and can produce undesired products that can further complicate the kinetic study [21].

### 2.1. Preparation of the V/γ-$Al_2O_3$ catalyst

Vanadium was deposited on γ-$Al_2O_3$ through adsorption, starting with 1000 ml of a 0.009 M solution of ammonium metavanadate (Strem Chemicals) which was put into contact with 1 g of γ-$Al_2O_3$ powder (Aldrich) for 48 h. The powder was then filtered, washed with 300 ml of deionised water (to remove the unbounded vanadium), dried at 353 K and finally calcined at 773 K for 5 h to stabilise the catalyst structure.

### 2.2. Catalyst characterisations

The particles of γ-$Al_2O_3$ supporting vanadium were spherical and about 100 μm in size, which was determined using a scanning electron microscope (SEM, Leica Stereoscan 440). Their specific surface area, estimated by adsorption–desorption of $N_2$ at 77 K using the BET method with an ASAP 2010 Micromeritics device, was found to be 258 $m^2\ g^{-1}$. The pore size distribution of γ-$Al_2O_3$ was very narrow with a mean diameter of 5.2 nm. The amount of vanadium on the γ-$Al_2O_3$ (1.12%, w/w) was determined by inductively coupled plasma (ICP), after treating the sample with hot aqua regia. Considering that a vanadia monolayer coverage corresponds to about $4.98 \times 10^{18}$ molecules of $V_2O_5$ per $m^2$ of specific surface area, the degree of coverage of the prepared catalyst was about 10% of that corresponding to a monolayer. Further studies on the supported vanadium were carried out by a transmission electron microscope (TEM, Jeol Jem 2010) equipped with an EDX probe: these observations revealed the excellent dispersion of the catalyst on the inert support and the absence of unwanted $V_2O_5$ aggregates, which favour overoxidation of propylene to carbon oxides.

### 2.3. Catalytic tests

A packed bed was prepared by mixing the catalysts with an inert material (SiC) in a 1:10 weight ratio. The solid mixture was put into a quartz reactor which was then put in an oven and homogeneously heated to temperatures up to 800 K. The feed flow rate was controlled by mass flow meters and helium was the inert carrier. Product streams were

Table 1
Some results of the criteria [22] applied in order to evaluate the influence of the undesired contribute to the intrinsic kinetic

| $T$ (°C) | Carberry $< 0.05/n$[a] | Weiz modulus | Hudgins $< 1/n$[a] | $D_{reactor}/d_{powder} > 10$ |
|---|---|---|---|---|
| 400 | $1.4 \times 10^{-6}$ | $1.7 \times 10^{-7}$ | $1.5 \times 10^{-6}$ | 140 |
| 480 | $7.96 \times 10^{-6}$ | $8.8 \times 10^{-7}$ | $7.9 \times 10^{-6}$ | 140 |

[a] The process was considered of first order ($n = 1$) with respect to propane concentration.

Table 2
Experimental conditions used for the kinetic measurements (catalytic bed weight = 2.1 g; SiC-catalytic powder ratio = 10)

| | X | | |
|---|---|---|---|
| | Propane | Propylene | Carbon monoxide |
| Space time ($g_{cat}$ s $ml^{-1}$) | 0.14 | 0.14 | 0.063 |
| Temperature range (°C) | 380–480 | 380–480 | 380–480 |
| $X/O_2$ range with [X] = constant | 0.7–20 | 0.12–0.6 | 0.53–1.87 |
| $X/O_2$ range with $[O_2]$ = constant | 1.1–19 | 0.15–0.75 | 0.15–0.75 |

analysed using gas chromatrography. Alkenes, alkanes and $CO_2$ were separated using a Porapack Q packed column (3 m long, 80/100 mesh) in a gas chromatograph (Perkin-Elmer 8700) equipped with a TCD. Oxygen and CO were analysed by a Carbosphere packed column (3 m long, 80/100 mesh) on a TCD (Perkin-Elmer Autosystem). Propylene, carbon monoxide and carbon dioxide were the only reaction products found (at the highest temperature a very small amount of ethylene was also detected, but in a negligible amount). The absence of oxygenate compounds was verified by a Carbowax packed column on a FID. The carbon mass balance was always less than 5%.

The first set of runs were carried out in order to determine kinetic limiting operating conditions. Propane conversion was measured by fixing the hydrocarbon–oxygen ratio in the feed and varying the amount of catalysts in the packed bed reactor. It is widely accepted that external diffusion can be excluded when the propane conversion curves overlap for two amounts of catalyst [22]. Fig. 2 shows that the contact times (defined in reference to the amount of catalytic powder) smaller than 0.3 $g_{cat}$ s $ml^{-1}$ should ensure kinetic conditions. In addition, a series of classical empirical checks [22] were also performed to evaluate the absence of temperature and concentration gradients, both outside and inside the catalytic particle. These checks are summarised in Table 1. It should be stressed that the parameters needed to perform the numerical calculation in Table 1 were either determined experimentally (reaction rate, particle diameter, particle porosity and tortuosity, reactant concentrations) or calculated through well-established empirical correlations (diffusivities, mass transfer coefficients).

Once the kinetic operating region was firmly established, experimental measurements of the reaction rates were carried out as follows: a total feed flow rate was set (1.5 ml $min^{-1}$ for the tests with hydrocarbons and 3.3 ml $min^{-1}$ for the carbon monoxide tests) and the ratio of the various reagents was changed for each run, as detailed in Table 2. Nine different concentration ratios were used for each data set. For each concentration ratio the results were the average of three analytical runs.

The low conversion measured proved that the reactor worked as a differential reactor, which allowed for easier data processing. For example, the following simple equation was used to calculate the rate of propane depletion:

$$-r_{C_3H_8} = -\frac{d[C_3H_8]}{d(W/F)} = \frac{(C_3H_8 \text{ molar flow rate})_{IN} - (C_3H_8 \text{ molar flow rate})_{OUT}}{\text{catalyst weight}} \quad (1)$$

The selectivity to propylene varied from greater than 90% at low conversion to 60% for higher conversion. Lower values of selectivity were not measured, even at less favourable conditions, i.e. low propane/oxygen molar ratio. Moreover, deactivation of the catalyst did not happen for more than 6 h (time generally required to complete a set of experimental measurements).

Data analysis was performed with commercial linear and non-linear regression routine software (Datafit 6.0, Oakdale Engineering, USA). The entry values used in the kinetic models were the exit concentration values.

## 3. Results and discussion

The determination of the kinetic parameters was carried out through independent experiments on some of the following reactions:

$$C_3H_8 + \tfrac{1}{2}O_2 \rightarrow C_3H_6 + H_2O \quad (2)$$

$$C_3H_8 + \tfrac{7}{2}O_2 \rightarrow 3CO + 4H_2O \quad (3)$$

$$C_3H_8 + 5O_2 \rightarrow 3CO_2 + 4H_2O \quad (4)$$

$$C_3H_6 + 3O_2 \rightarrow 3CO + 3H_2O \quad (5)$$

$$C_3H_6 + \tfrac{9}{2}O_2 \rightarrow 3CO_2 + 3H_2O \quad (6)$$

$$CO + \tfrac{1}{2}O_2 \rightarrow CO_2 \quad (7)$$

Simultaneous and consecutive reactions occur alongside the principal reaction (2), the oxidative dehydrogenation of propane.

Assuming a power law type rate for each of the above reactions, the overall rate of formation for the four components

considered is:

$$-r_{C_3H_8} = -\frac{d[C_3H_8]}{d(W/F)} = k_1[C_3H_8]^a[O_2]^b + k_2[C_3H_8]^c[O_2]^d + k_3[C_3H_8]^e[O_2]^f \quad (8)$$

$$r_{C_3H_6} = \frac{d[C_3H_6]}{d(W/F)} = k_1[C_3H_8]^a[O_2]^b - k_4[C_3H_6]^g[O_2]^h - k_5[C_3H_6]^i[O_2]^l \quad (9)$$

$$r_{CO} = \frac{d[CO]}{d(W/F)} = 3k_2[C_3H_8]^c[O_2]^d + 3k_4[C_3H_6]^g[O_2]^h - k_6[CO]^m[O_2]^n \quad (10)$$

$$r_{CO_2} = \frac{d[CO_2]}{d(W/F)} = 3k_3[C_3H_8]^e[O_2]^f + 3k_5[C_3H_6]^i[O_2]^l + k_6[CO]^m[O_2]^n \quad (11)$$

Eighteen parameters (kinetic constants and reaction orders) need to be determined for each temperature investigated. Given the very high number of undetermined parameters, we used a "cascade" approach, where two simpler reaction systems were studied and experimentally defined. In detail, the procedure was as follows:

- Determination of the kinetic constant and reaction orders for the combustion of carbon monoxide (reaction (7) or sub-scheme (a) in Fig. 1).
- Determination of the kinetic constants and reaction orders for the combustion of propylene (reactions (5)–(7) or sub-scheme (b) in Fig. 1).
- Determination of all the other kinetic constants and reaction orders.

Each of the above-mentioned steps will be now considered in detail. The oxidation of carbon monoxide to carbon dioxide will be considered (sub-scheme (a) in Fig. 1):

$$CO + \tfrac{1}{2}O_2 \rightarrow CO_2 \quad (12)$$

$$r_{CO_2} = \frac{d[CO_2]}{d(W/F)} = k_6[CO]^m[O_2]^n \quad (13)$$

Using the Arrhenius equation

$$k_6 = k_{06}\exp\left(\frac{-E_{a6}}{RT}\right) \quad (14)$$

the expression for the rate of carbon monoxide in logarithmic form becomes:

$$\ln(-r_{CO}) = \ln k_{06} + m\ln[CO] + n\ln[O_2] - \frac{E_{a6}}{RT} \quad (15)$$

For a constant reagent composition

$$\ln(-r_{CO}) = k' - \frac{E_{a6}}{RT} \quad (16)$$

Therefore, the activation energy, $E_{a6}$, was obtained by carrying out a series of runs at a constant reagent composition, varying the temperature and then by plotting the measured reaction rate as a function of the inverse temperature (as shown in Fig. 3).

Reaction orders for the same system were obtained by carrying out a further series of runs at constant temperature and different $CO/O_2$ ratios. Fig. 4 depicts the experimental results (for one specific temperature) and the best-fit straight line used for the determination of the reaction orders relative to the two reagents. The reaction orders were then simply estimated by averaging the values obtained for each single temperature.

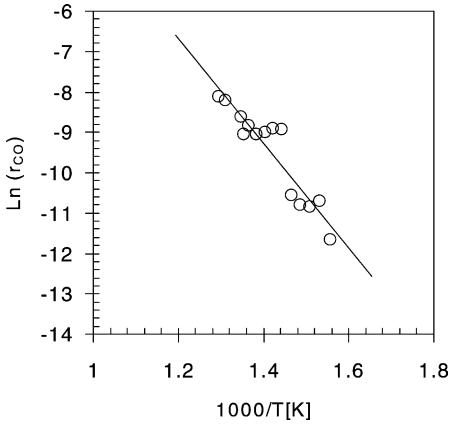


Fig. 3. Arrhenius plot of the CO depletion rate during combustion to $CO_2$.

The second reaction (considered independently) is the combustion of propylene. The assumed reaction system is reported in Fig. 1 (sub-scheme (b)) and only reactions (5)–(7) need to be considered at this stage. Given that the kinetic parameters relative to the combustion of carbon monoxide to carbon dioxide ($k_6$, $m$, $n$) have already been estimated, it was easy to see that $k_4$, $g$ and $h$ could be obtained from a balance of carbon monoxide (Eq. (10)) and $k_5$, $i$ and $l$ from a balance of carbon dioxide (Eq. (11)). These kinetic constants and reaction orders were experimentally estimated by feeding the reactor a mixture of propylene and oxygen. Data treatment was very much similar to the one given for the previous combustion of carbon monoxide and will not be repeated here for sake of brevity.

Finally, the overall reaction was considered and all the remaining parameters were estimated by using the results of the two previous reported reactions and carrying out the oxidation of propane–oxygen mixtures ($k_1$, $a$ and $b$ from a mass balance on propylene (Eq. (9)); $k_2$, $c$ and $d$ from CO balance (Eq. (10)) and $k_3$, $e$ and $f$ from a $CO_2$ balance (Eq. (11)).

Table 3 summarises all the estimated values with a 95% confidence interval, the order of reactions reported are the average of those calculated at the various investigated

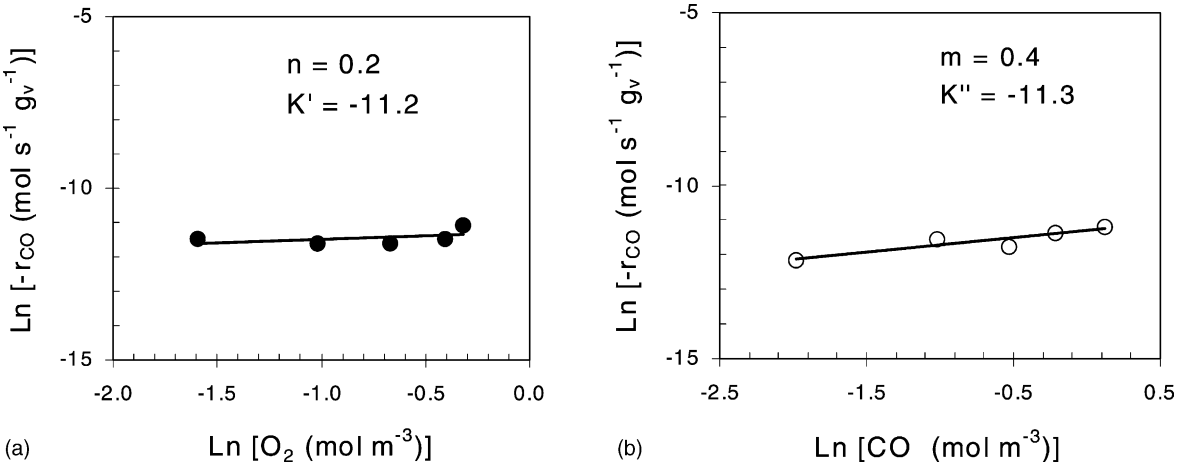


Fig. 4. Logarithmic plots of the CO consume rate as a function of oxygen (a) or CO concentration (b). Temperature: 400 °C.

temperatures; their variation was always very small and attributable to experimental error. The validity of the estimation exercises can be seen in Fig. 5, where calculated and actual experimental data is compared in terms of both the rate of propane depletion and process yield calculated as the product between selectivity and conversion. The simple power law kinetic rate yields an agreement of 16% on average with a maximum percent error of 28%.

There are various considerations that can be made from the analysis of Table 3. Firstly, it should be noted that the constants $k_2$ and $k_3$ were estimated to be equal to 0, because the estimated values were found to be smaller than their confidence limits. Consequently, the direct formation of carbon monoxide and carbon dioxide from propane can be ignored. This fact is probably related to the preparation conditions of the catalyst (concentration of the metavanadate solution, pH and calcination temperature), suggesting the presence of tetrahedral vanadate species (either isolate or also as polyvanadates) on the $\gamma$-$Al_2O_3$ [19]. How the surrounding environment and co-ordination of vanadium contributes to the process selectivity is still being debated in spite of numerous studies.

Reaction order values indicate that the overall kinetic rate is more influenced by the hydrocarbon (partial orders *a*, *g*, *i*) rather than the oxygen concentration (partial orders *b*, *h*, *l*). The formation rate curves (Fig. 6) extrapolated to zero oxygen concentration seem to have intercepts. This does not seem to happen for the rate formation curves of propane, as

Table 3
Kinetic parameters estimated for the power law model

| | Value ± confidence limits (95%) | | | | |
|---|---|---|---|---|---|
| | 380 °C | 400 °C | 420 °C | 450 °C | 480 °C |
| $k_1$ $((m^3)^{a+b}\,mol^{1-(a+b)}\,(g_{cat})^{-1}\,s^{-1})$ | $(1.1 \pm 0.1) \times 10^{-5}$ | $(1.7 \pm 0.6) \times 10^{-5}$ | $(2.7 \pm 0.9) \times 10^{-5}$ | $(5.0 \pm 0.2) \times 10^{-5}$ | $(8.9 \pm 0.9) \times 10^{-5}$ |
| $k_2$ $((m^3)^{c+d}\,mol^{1-(c+d)}\,(g_{cat})^{-1}\,s^{-1})$ | – | – | – | – | – |
| $k_3$ $((m^3)^{e+f}\,mol^{1-(e+f)}\,(g_{cat})^{-1}\,s^{-1})$ | – | – | – | – | – |
| $k_4$ $((m^3)^{g+h}\,mol^{1-(g+h)}\,(g_{cat})^{-1}\,s^{-1})$ | $(2.7 \pm 1) \times 10^{-5}$ | $(4.3 \pm 0.6) \times 10^{-5}$ | $(4.7 \pm 0.1) \times 10^{-5}$ | $(1.2 \pm 0.1) \times 10^{-4}$ | $(2.1 \pm 0.02) \times 10^{-4}$ |
| $k_5$ $((m^3)^{i+l}\,mol^{1-(i+l)}\,(g_{cat})^{-1}\,s^{-1})$ | $(1.5 \pm 0.6) \times 10^{-5}$ | $(1.7 \pm 0.6) \times 10^{-5}$ | $(2.1 \pm 0.3) \times 10^{-5}$ | $(2.7 \pm 0.5) \times 10^{-5}$ | $(3.3 \pm 0.05) \times 10^{-5}$ |
| $k_6$ $((m^3)^{m+n}\,mol^{1-(m+n)}\,(g_{cat})^{-1}\,s^{-1})$ | $(9.4 \pm 0.1) \times 10^{-6}$ | $(1.8 \pm 0.1) \times 10^{-5}$ | $(3.3 \pm 0.2) \times 10^{-5}$ | $(7.8 \pm 0.1) \times 10^{-5}$ | $(1.7 \pm 0.1) \times 10^{-4}$ |
| *a* | 0.59 ± 0.06 | | | | |
| *b* | 0.26 ± 0.01 | | | | |
| *c*, *d*, *e*, *f* | – | | | | |
| *g* | 0.42 ± 0.07 | | | | |
| *h* | 0.29 ± 0.03 | | | | |
| *i* | 0.87 ± 0.05 | | | | |
| *l* | 0.05 ± 0.02 | | | | |
| *m* | 0.40 ± 0.06 | | | | |
| *n* | 0.20 ± 0.06 | | | | |
| $E_{a1}$ (kJ mol$^{-1}$) | 87 ± 41 | | | | |
| $E_{a2}$, $E_{a3}$ (kJ mol$^{-1}$) | – | | – | | |
| $E_{a4}$ (kJ mol$^{-1}$) | 84 ± 42 | | | | |
| $E_{a5}$ (kJ mol$^{-1}$) | 34 ± 12 | | | | |
| $E_{a6}$ (kJ mol$^{-1}$) | 119 ± 58 | | | | |

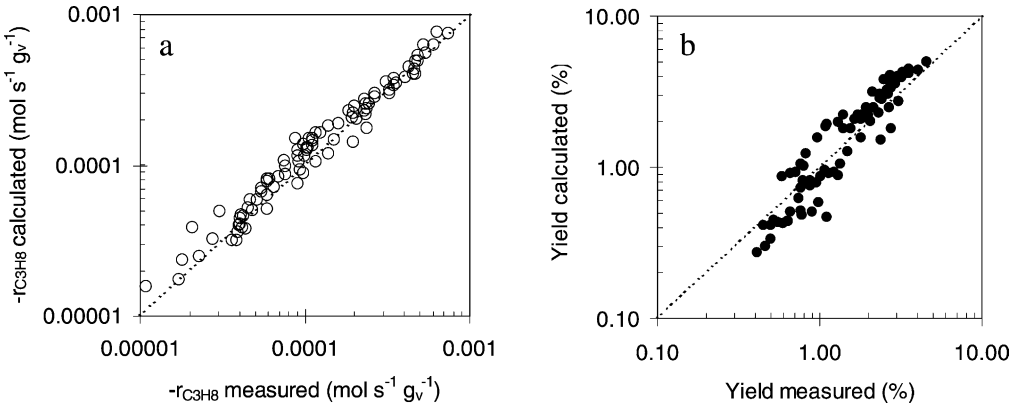


Fig. 5. Parity plot of: (a) the observed and calculated propane depletion rate using the kinetic parameters reported in Table 3 and (b) the experimental and calculated yield on the basis of the power law kinetic model.

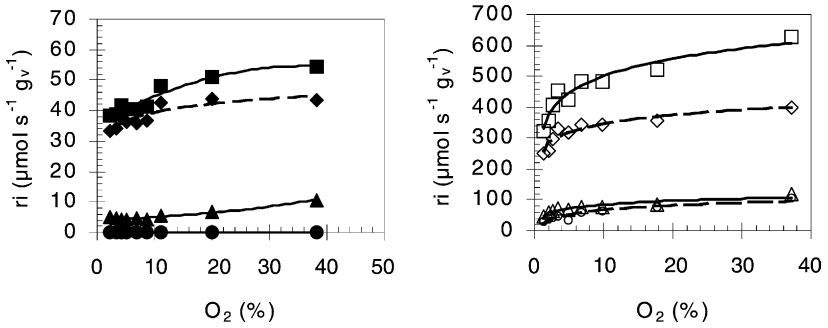


Fig. 6. Effect of the oxygen concentration on the product formation rate and on the depletion rate of propane at $T = 380\,^{\circ}C$ (full symbols) and $T = 480\,^{\circ}C$ (empty symbols): $-r_{C_3H_8}$ (■), $r_{C_3H_6}$ (◆), $r_{CO_2}$ (▲), $r_{CO}$ (●).

reported in Fig. 7. Moreover, the higher the propane concentration, the higher the propylene formation rate is, but the higher the propylene concentration, the greater is the combustion reaction (6). This behaviour suggests that the partial pressure of $O_2$ has a little influence on the rate-determining step of the mechanism. This agrees with the conclusions and mechanisms of other authors for other catalytic systems [23]. As the reaction of catalyst regeneration by gaseous oxygen is much faster than that of product formation, the overall process rate is only slightly influenced by the gaseous oxygen concentration. This is demonstrated by the experimental reaction order in the region of 0.1–0.2 in Table 3.

Creaser et al. [11] studied oxygen dependence and showed that the lower the oxygen partial pressure, the higher the propylene selectivity is. This is probably related to the fact that lattice oxygen is always available, even at low oxygen partial pressure. Thus, to observe an oxygen kinetic dependence, very low oxygen partial pressure must be used, which also influences the vanadium oxidation state. Moreover, as said in [6], the hydrocarbon oxygen ratio is the fundamental

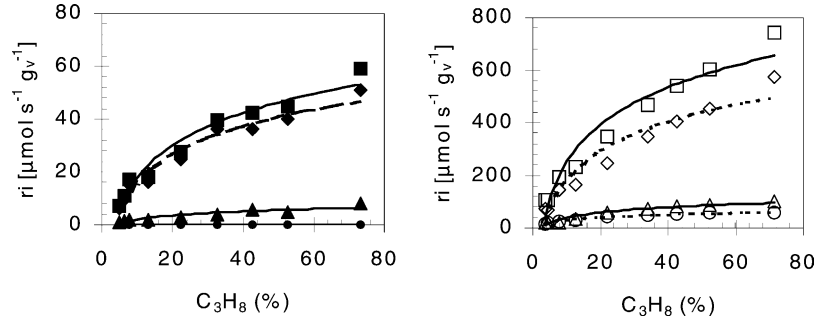


Fig. 7. Effect of the propane concentration on the product formation rate and on the depletion rate of propane at $T = 380\,^{\circ}C$ (full symbols) and $T = 480\,^{\circ}C$ (empty symbols): $-r_{C_3H_8}$ (■), $r_{C_3H_6}$ (◆), $r_{CO_2}$ (▲), $r_{CO}$ (●).

variable in the reconstruction of the catalytic site, since it influences the ratio between oxidation and reduction rates of the catalytic site and drives the selectivity toward propylene or combustion products [24]. Creaser and Andersson [8] have studied the kinetic of propane oxidehydrogenation over a VMgO catalyst hypothesising only reactions (2), (5) and (6), while neglecting reaction (7). This scheme is very similar to the one found by us. Their partial reaction orders for reactions (1) and (4) ($a = 0.53$, $b = 0.29$, $g = 0.38$, $h = 0.17$) are very close to those found in our elaboration. The apparent activation energies found by these authors are higher than those found in the present study (e.g. for reaction (2), $E_a$ is about 124 kJ mol$^{-1}$) but this is because the catalyst they studied is active in an higher temperature range.

Several considerations were made about a possible mechanism with a simple rate equation for the ODH of propane, and three schemes (with their corresponding rate equations) were considered: (a) propane and oxygen is adsorbed on the catalyst surface where they react to give propylene (the typical Langmuir–Hinshelwood approach); (b) oxygen from the gas phase reacts with propane adsorbed on the catalyst surface (the typical Eley Rideal approach); (c) propane is adsorbed on the catalyst surface and oxygen re-oxidises the reduced catalytic site which in turn reacts with the adsorbed propane to give propylene (the redox approach). Approaches (a) and (b) were discarded because their rate expressions contrasted with the experimental data. The redox mechanism was further investigated because it seemed to agree better with the previous kinetic considerations.

Molecular oxygen takes part in the reaction by re-oxidising the catalytic site. This was previously reduced via a surface reaction from the adsorbed propane to adsorbed propylene:

$$C_3H_8 + \sigma_{ox} \leftrightarrow C_3H_8 * \sigma_{ox} \quad \text{(propane adsorption)} \quad (17)$$

$$C_3H_8 * \sigma_{ox} + \sigma_{rid} \rightarrow C_3H_6 * \sigma_{rid} + H_2O * \sigma_{rid} \quad \text{(surface reaction and site reduction)} \quad (18)$$

$$C_3H_6 * \sigma_{rid} \leftrightarrow C_3H_6 + \sigma_{rid} \quad \text{(propene desorption)} \quad (19)$$

$$H_2O * \sigma_{rid} \leftrightarrow H_2O + \sigma_{rid} \quad \text{(water desorption)} \quad (20)$$

$$\sigma_{rid} + 0.5O_2 \leftrightarrow \sigma_{ox} \quad \text{(site re-oxidation)} \quad (21)$$

The following kinetic equation was obtained by considering the very quick desorption rate of both water and propylene (Eqs. (19) and (20)), the steady-state condition for reactions (17) and (20), and reaction (18) as the rate-determining step:

$$r_{17} = \frac{K_{tot}[C_3H_8][O_2]^{0.5}}{1 + K_{eq21}[O_2]^{0.5} + (K_{eq17}K_{eq21}[C_3H_8][O_2]^{0.5})} \quad (22)$$

where $K_{tot} = k_{18}K_{eq17}K_{eq21}$, $k_{18}$ (mol s$^{-1}$ g$^{-1}$) is the kinetic constant for the reaction (18), $K_{eq17}$ and $K_{eq21}$ are the equilibrium constants for reactions (17) and (20), respectively, expressed in $(m^3\,mol^{-1})^{1.5}$ and $(m^3\,mol^{-1})^{0.5}$. Concentrations were expressed in mol m$^{-3}$.

In order to evaluate the constants in the above-mentioned rate expression, Eq. (22) was linearised for both the constant oxygen and propane concentration cases. When oxygen was considered constant the equation becomes:

$$\frac{1}{r_{18}} = \frac{1 + b'}{a'[C_3H_8]} + \frac{c'}{a'} \quad (23)$$

where $a' = K_{tot}[O_2]^{0.5}$, $b' = K_{eq17}[O_2]^{0.5}$ and $c' = K_{eq17}K_{eq21}[O_2]^{0.5}$.

When propane concentration was kept constant, the following equation was used:

$$\frac{1}{r_{18}} = \frac{1}{a''[O_2]^{1/2}} + \frac{K_{eq20} + c''}{a''} \quad (24)$$

where $a'' = K_{tot}[C_3H_8]$ and $c'' = K_{eq17}K_{eq21}[C_3H_8]$.

By using the above equations, initial estimates of the constants were obtained and used to calculate the values more accurately by non-linear regression analysis.

The final values obtained are reported in Table 4 whereas the comparison between experimental and calculated rates are depicted in Fig. 8. The fair agreement (with only 17% relative error) shown in Fig. 8 indicates how well the mechanism suggested here interprets the experimental data. The kinetic constant of the surface reaction (18), $k_{18}$, grows as

Table 4
Kinetic parameters estimated for the redox model

| $T$ (°C) | $k_{18} \times 10^4$ (mol s$^{-1}$ g$^{-1}$) | $K_{17}$ (m$^3$ mol$^{-1}$) | $K_{21} \times 10^2$ (m$^{3/2}$ mol$^{-1/2}$) |
|---|---|---|---|
| 380 | 3.2 | 560.7 | 1.3 |
| 400 | 4.3 | 306.4 | 1.8 |
| 420 | 5.5 | 173.4 | 2.6 |
| 450 | 7.9 | 78.3 | 4.1 |
| 480 | 11.0 | 37.7 | 6.3 |

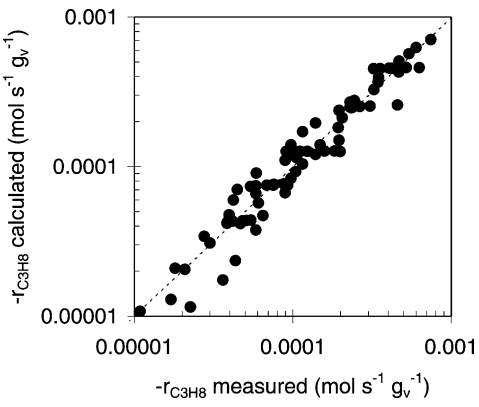


Fig. 8. Parity plot of the observed and calculated propane depletion rate using the redox model.

the temperature increases with an activation energy of about $50\,kJ\,mol^{-1}$. The equilibrium constant $K_{17}$ decreases as the temperature increases and highlights the exothermic character ($\Delta H_{ads} = -110\,kJ\,mol^{-1}$) of propane adsorption on the catalytic site (reaction (17)). The process of re-oxidation of the catalytic site through molecular oxygen was improved as the temperature increased (shown in Table 4 for $K_{21}$). This behaviour presents an analogy with other systems reported in literature [1,23].

Finally, in agreement with literature data [6], the kinetic for site re-oxidation is greater than that of the actual chemical reaction, thus confirming that the oxygen in the gas only slightly influences the overall rate.

## 4. Conclusions

The kinetic of propane ODH on a V/γ-$Al_2O_3$ catalyst prepared by the adsorption technique was studied. Two approaches were applied. In the first one, power law expressions were used to describe the network of reactions involving propane, propylene, CO and $CO_2$. The information obtained in this way could be useful for engineering purposes and we will try to use it to optimise a model of a catalytic membrane reactor, to be used in the ODH of propane.

In the second approach, the experimental data was fitted with a rate equation obtained by assuming that molecular oxygen re-oxidises the active site reduced by the surface reaction.

## Acknowledgements

This work was financially supported by Ministero dell'Università e della Ricerca (MIUR, Cofin 1999) and by Snamprogetti SpA.

## References

[1] J.M. Thomas, W.J. Thomas, Principles and Practice of Heterogeneous Catalysis, VCH, Weinheim, FRG, 1997.
[2] D. Wolf, N. Dropka, Q. Smejkal, O. Buyevskaya, Oxidative dehydrogenation of propane for propylene production—comparison of catalytic processes, Chem. Eng. Sci. 56 (2001) 713.
[3] J. Cosyns, J. Chordorge, D. Commereuc, B. Torck, Maximize propylene production, Hydrocarbon Process. 61 (1998) 22.
[4] G. Centi, F. Cavani, F. Trifirò, Selective Oxidation by Heterogeneous Catalysis, Kluwer Academic Publishers, New York, 2001.
[5] F. Cavani, F. Trifirò, The oxidative dehydrogenation of ethane and propane as an alternative way for the production of light olefins, Catal. Today 24 (1995) 307.
[6] E.A. Mamedov, V. Cortés Corberàn, Oxidative dehydrogenation of lower alkanes on vanadium oxide-based catalyst. The present state of the art and outlooks, Appl. Catal. A 127 (1995) 1.
[7] T. Blasco, J.M. Lopez Nieto, Oxidative dehydrogenation of short chain alkanes on supported vanadium oxide catalyst, Appl. Catal. A 157 (1997) 117–142.
[8] D.C. Creaser, B. Andersson, Oxidative dehydrogenation of propane over V–Mg–O: kinetic investigation by nonlinear regression analysis, Appl. Catal. A 141 (1996) 131.
[9] A. Khodakov, J. Jang, S. Su, E. Iglesia, A.T. Bell, Structure and properties of vanadium oxide-zirconia catalysts for propane oxidative dehydrogenation, J. Catal. 177 (1998) 343.
[10] F. Genser, S. Pietrzyk, Oxidative dehydrogenation of propane on $V_2O_5/TiO_2$ catalysts under transient conditions, Chem. Eng. Sci. 54 (1999) 4315.
[11] D.C. Creaser, B. Andersson, R.R. Hudgins, P.L. Silveston, Kinetic modelling of oxygen dependence in oxidative dehydrogenation of propane, Can. J. Chem. Eng. 78 (2000) 182.
[12] K. Chen, A.T. Bell, E. Iglesia, Kinetics and mechanism of oxidative dehydrogenation of propane on vanadium, molybdenum, and tungsten oxides, J. Phys. Chem. B 104 (2000) 1292.
[13] N. Boisdron, A. Monnier, L. Jalowlcki-Duhamel, Y. Barabaux, Oxydehydrogenation of propane on $V_2O_5/TiO_2$ catalyst: kinetic and mechanistic aspects, J. Chem. Soc., Faraday Trans. 91 (1995) 2899.
[14] A. Khodakov, B. Olthof, A.T. Bell, E. Iglesia, Structure and catalytic properties of supported vanadium oxides: support effects on oxidative dehydrogenation reactions, J. Catal. 181 (1999) 205.
[15] R. Grabowski, B. Grzybowska, K. Wcislo, Properties of $V_2O_5/TiO_2$ catalytic system with alkali metal cations in oxidative dehydrogenation of propane and isopropanol decomposition, Pol. J. Chem. 68 (1994) 1803.
[16] M. Baldi, E. Finocchio, C. Pistarino, G. Busca, Evaluation of the mechanism of the oxydehydrogenation of propane over manganese oxide, Appl. Catal. A 173 (1998) 61.
[17] M. Santel, G. Thomas, A. Kadduri, C. Mazzocchia, R. Anoucinsky, Kinetics of oxidative dehydrogenation of propane on β-phase of nickel molybdate, Appl. Catal. 155 (1997) 217.
[18] D. Stern, R. Grasselli, Reaction network and kinetics of propane oxidehydrogenation over nickel cobalt molybdate, J. Catal. 167 (1996) 560.
[19] J.G. Eon, R. Olier, J.C. Volta, Oxidative dehydrogenation of propane on γ-$Al_2O_3$ supported vanadium oxides, J. Catal. 145 (1994) 318.
[20] H.S. Fogler, Elements of Chemical Reaction Engineering, third ed., Prentice-Hall, New Jersey, 1999.
[21] V.P. Vislovskiy, T.E. Suleimanov, M.Y. Sinev, Y.P. Tulenin, L.Y. Margolis, V. Cortés Corberàn, On the role of heterogeneous and homogeneous processes in oxidative dehydrogenation of $C_3$–$C_4$ alkanes, Catal. Today 61 (2000) 287.
[22] J.C. Schaltter (Ed.), A Practical Guide to Catalyst Testing, Study No. 4186TE, Catalytica Studies Division, Mountain-View, 1987.
[23] P.J. Gellins, H.J.M. Bouwmeester, Solid state aspects of oxidation catalysis, Catal. Today 58 (2000) 1.
[24] A. Bottino, G. Capannelli, A. Comite, Catalytic membrane reactors for the oxidehydrogenation of propane: experimental and modelling study, J. Membr. Sci. 197 (2002) 75.